FACTA UNIVERSITATIS
Series: **Mechanical Engineering** Vol. 22, Nº 4, 2024, pp. 759 - 772
https://doi.org/10.22190/FUME240118018Y

Original scientific paper

ATTENUATION CHARACTERISTICS OF ULTRASONIC WAVES FROM SONAR LOGGING TOOLS IN SALT CAVERN GAS STORAGE

Hai-Yan Yang[1], Yu Wang[1], Sen-Lin Liu[1], Qing Tu[2], Gang Chen[1]

[1]School of Mechanical Engineering, Xihua University, Sichuan, China
[2]Chengdu Technological University, School of Intelligent Manufacturing, Chengdu, Sichuan, China

ORCID iDs: Hai-Yan Yang https://orcid.org/0000-0003-4363-505X
Yu Wang https://orcid.org/0000-0001-5147-7931
Sen-Lin Liu https://orcid.org/0009-0007-7626-8731
Qing Tu https://orcid.org/0000-0003-3332-2412
Gang Chen https://orcid.org/0009-0005-4919-7830

Abstract. *The sonar detection of salt cavern gas storage (SCGS) has a low accuracy due to sound wave attenuation. To solve the problem, this paper analyzes the attenuation features of sound waves in SCGS, based on the mechanical wave equation and Urick sound wave attenuation theory, as well as expression of sound velocity in dilute solution and the general empirical formula of solution density. Specifically, three attenuation forms of sound waves in dilute solutions with different concentrations were studied, and a theoretical model for the total attenuation of sound waves in SCGS was established. The model was adopted to explore the effect of solution temperature and concentration on sound wave attenuation. The results yield some interesting findings. It is shown that the temperature has a small overall effect on the attenuation of sound waves. Also, the total attenuation coefficient of sound waves in suspensions with different concentrations increases with the frequency of the sound waves. Furthermore, when the frequency of the sound waves remains unchanged, the total attenuation coefficient increases with the concentration of the suspension. Finally, when the solution concentration is less than 10%, the total attenuation coefficient of the sound waves depends on scattering attenuation, and the sound wave attenuation is not greatly affected by the viscous attenuation and thermal attenuation. Four salt solutions were tested to verify the correctness of the theoretical research. The experimental results show that, in the SCGS environment, the salt solutions are ranked in a descending order of the influence over sonar detection accuracy starting from potassium chloride solution, via magnesium sulfates solution and calcium chloride solution to sodium chloride solution. The research provides a strong theoretical guidance for sonar detection of SCGS, and a powerful engineering reference for sonar detection in brine.*

Key words: *Salt cavern gas storage, Sonar detection, Acoustic attenuation, Brine, Wave frequencies*

Received: January 18, 2024 / Accepted April 11, 2024
Corresponding author: Yu Wang
School of Mechanical Engineering, Xihua University, 9999 Hongguang Avenue, Pidu District, Chengdu City, Sichuan Province 611730, China.
E-mail: xhwangyu@yeah.net

1. INTRODUCTION

Natural gas, as a clean and efficient low-carbon fossil energy, has experienced explosive growth in consumption. It is of particular importance to ensure the supply of natural gas through peak regulation. An underground gas storage offers an effective means of natural gas peak regulation. Such an underground gas storage is mainly deployed in halite and other underground rock layers, which feature extremely low porosity and permeability, as well as stable mechanical properties [1].

Halite is internationally recognized as the best place for energy storage [2]. However, salt cavern gas storage (SCGS) often has a complex internal environment, and lies deep underground. The cavity may creep and collapse, exerting a great impact on the shape of the dissolved cavity of the underground gas storage. To ensure the security of SCGS, it is extremely important to track the shape of the salt cavern in real time, and regularly explore and evaluate the shape of the dissolved cavity.

Currently, ultrasonic detection is the most popular way to detect the shape of SCGS. But the detection accuracy would be significantly affected by the water and various salt media inside SCGS. The main effect is the attenuation of ultrasonic waves. Hence, the key and difficulty of ultrasonic detection are to clarify the attenuation features of ultrasonic waves in the gas storage media.

Ultrasonic wave attenuation in solutions can be divided into three forms: viscous attenuation, thermal attenuation, and scattering attenuation. Harker et al. [3] discussed the scattering theory of compression waves in viscous fluids, and deduced the variation of ultrasonic phase velocity and attenuation with the changes of fluid viscosity, particle, elastic modulus, and concentration. Prek [4] proposed a method to determine the acoustic wave characteristics in an elastoplastic fluid-filled tube using the frequency domain analysis and applied it to calculate the acoustic wave number from a transfer function between three pressure measuring devices, which showed that the acoustic wave number was complex and related to the wave speed and decay rate. Ross [5] studied the propagation of ultrasonic waves in multi-layer media, composite materials and viscoelastic materials, and created the three-media viscous attenuation model for ultrasonic waves in multi-layer media. Queiros et al. [6] explored the velocity and attenuation of sound waves in anisotropic materials. After solving the cross-correlation of the transmitted and received signals, they performed sinusoidal fitting on the two signals, measured the sound velocity with high precision, and constructed a comprehensive finite-element model for two kinds of defects. Hutchinson and Bevis [7] found that, as the heating temperature of low carbon steel rises, the enhancement of ferrite crystal anisotropy and the subsequent phase transformation at high temperature will lead to an attenuation peak of sound wave, which is consistent with Rayleigh zone attenuation theoretical model. Through experiments, Hutchins et al. [8] weakened the sound signal attenuation induced by scattering and viscoelastic effects, using piezoelectric composite transducers and pulse compression processing. Li et al. [9] investigated the attenuation of ultrasound in composites and proposed a time-domain analysis method for the propagation of ultrasound waves based on the finite element analysis of a bilayer fiber/matrix. The results show that the interfacial energy dissipation of the acoustic wave is the main factor affecting the ultrasonic attenuation characteristics. Based on the Epstein-Carhart-Allegra-Hawley (ECAH) scattering model, Tsuji et al. [10] constructed a technique called multiple echo reflection ultrasonic spectroscopy, which makes the viscoelastic ECAH model applicable when the particle size and wavelength are comparable. Yu et al. [11] proposed a method

to measure the concentration of hydrate-water dispersion particles based on multi-frequency ultrasonic attenuation. The ultrasonic scattering attenuation model that accounts for multiple scattering was developed to predict the attenuation of liquid-solid dispersions. Zhao et al. [12] developed a new predictive model for the ultrasonic attenuation of spherically mixed particles in gaseous media using the Monte Carlo method. The numerical simulation results for the system with a single particle type are in good agreement with the results of various standard models, such as classical ECAH model and McC model. Through investigation and analysis, it can be seen that the propagation process of sound waves in the salt cavern environment is complex, involving regional differences. Therefore, it is an urgent problem to master the attenuation features of sound waves in SCGS media.

Starting with the attenuation form of ultrasonic waves in complex environment, this paper analyzes the main attenuation modes of ultrasonic waves in SCGS environment. According to the wave equation and the specific environment of gas storage, the authors established the theoretical relationship of ultrasonic attenuation in SCGS, carried out orthogonal analysis of the three attenuation forms to grasp the change features of ultrasonic attenuation with SCGS medium and ultrasonic excitation frequency. In addition, the theoretical results were verified through experiments, providing a strong theoretical guidance for the sonar detection of SCGS.

2. WAVE EQUATION

Ultrasound, as a mechanical wave, is essentially a mechanical vibration propagating in a continuous medium. The wave equation for a non-ideal medium can be expressed as [13]:

$$\frac{\partial^2 p}{\partial x^2} = \frac{1}{c^2}\frac{\partial^2 p}{\partial t^2} \tag{1}$$

where, $c = \left(\frac{k_s}{\rho}\right)^{\left(\frac{1}{2}\right)}$, ρ is the density of the medium, k_s=$-v\frac{dP}{dV}$ and it is the elastic modulus of the insulator, V is the volume, x is the propagation distance, t is the propagation time, p is the sound pressure and ξ is the displacement. Hence, $p = k_s * \frac{dV}{V}$, and $\frac{dV}{V} = \frac{d\xi}{dx}$.

Since the propagating medium in the salt cavern is a solid-liquid mixture, the adjacent particles in the propagating medium do not move at the same velocity. According to Newton's law of internal friction in fluid mechanics, the viscous force per unit area of a one-dimensional (1D) planar wave with the dynamic viscosity of η can be expressed as:

$$T' = \eta\frac{\partial v}{\partial x} \tag{2}$$

Therefore, the acoustic equation can be written as:

$$\rho\frac{\partial^2 \xi}{\partial t^2} = K_s\frac{\partial^2 \xi}{\partial x^2} + \eta\frac{\partial^3 \xi}{\partial x^2\,\partial t} \tag{3}$$

Here, K_s is the adiabatic volume elasticity coefficient of the fluid. For simple harmonic waves, the general solution of differential Eq. (3) is usually represented by a combination of complex numbers. Let α_η be the sound absorption coefficient under viscous fluid. Then, the wave equation of sound waves under non-ideal conditions can be obtained as:

$$\xi = \xi_0 e^{-\alpha_\eta x} e^{j\omega\left(t-\frac{x}{c}\right)} \tag{4}$$

The medium inside the underground cavity is very complex. In such an environment, the attenuation mechanism of sound waves is often the combined effect of multiple attenuation mechanisms. As shown in Fig. 1, during the actual propagation, the sound wave would experience viscous attenuation due to the internal friction of the medium, scattering attenuation due to the undissolved medium, and thermal attenuation due to the heat conduction [14-17].

This study intends to adopt the sound velocity and sound attenuation coefficient derived in the Urick model [18], and explore the case of dilute solutions within 10%, without considering insoluble particles.

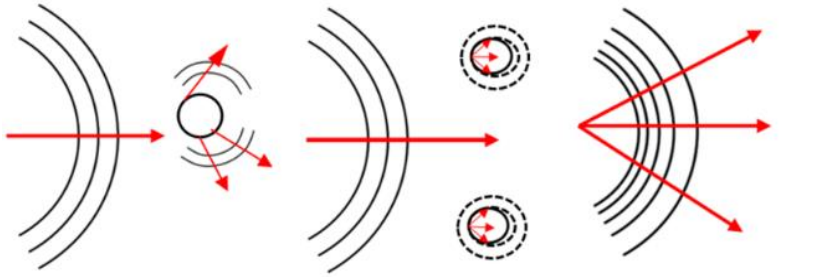

Fig. 1 Schematic diagram of acoustic attenuation in complex environment

3. ATTENUATION FEATURE ANALYSIS

3.1. Viscous Attenuation Features

Based on Urick model [18], the sound velocity in suspensions can be expressed as:

$$c = \left(P_{\text{eff}}\beta_{eff}\right)^{-1/2} \tag{5}$$

$$P_{eff} = \rho(1-\varphi) + p'\varphi \tag{6}$$

$$\beta_{eff} = \beta_c(1-\varphi) + \beta_c'\varphi \tag{7}$$

where, P_{eff} is the effective density, β_{eff} is the compression coefficient, φ is the liquid concentration, p' is the particle density, β_c' is the isothermal compression coefficient of solid particles and β_c is the liquid isothermal compression coefficient.

Eqs. (5-7) show that the velocity of the sound wave decreases with the rise of concentration. Also, with a higher the particle density, the sound velocity is slower and the velocity decreases faster. According to Yang et al. [19], this paper adopts the empirical relationship between the density of the solution, the mass content of the substance, and the temperature:

$$\rho = 1006.0 + 737.7C - 0.311T - 1.993 \times 10^{-3}T^2 \tag{8}$$

where, C is the solute mass fraction and T is the absolute temperature. The formula was analyzed to calculate the change of solution density when the temperature is in the range

between 0°C and 100°C and the mass fraction of solute falls between 0% and 10%. The calculation results are shown in Fig. 2.

It can be seen from Fig. 2 that the density of the solution changes with the temperature and the mass fraction of the solute. The higher the temperature, the smaller the density of the solution. But the density decrement is quite small. The temperature rise of 120°C only leads to 6.5% decline in solution density. By contrast, the solute mass fraction has a large impact on solution density: the solution becomes 18% denser, as the mass fraction of the solute grows by 25%. Under the joint influence of temperature and solute mass fraction, the solute mass fraction has a greater impact on the solution density than the temperature. In the subsequent analysis, the solution density and sound wave attenuation are investigated, in view of the solute mass fraction and solution temperature.

The liquid concentration normally grows exponentially with its viscosity. This paper fits the relationship between the two factors as a quadratic equation:

$$\eta = 10\varphi^2 \tag{9}$$

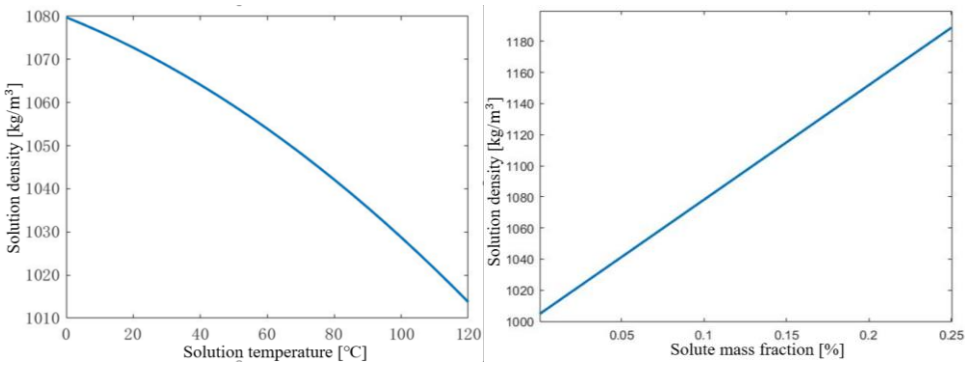

Fig. 2 The relationship between solution density, temperature and solute mass fraction

The viscous attenuation coefficient of the sound wave derived from the Navier-Stokes (N-S) equation can be expressed as:

$$\alpha_\eta = \frac{2\pi^2 f^2 \eta}{\rho c^3} \tag{10}$$

where, f is the frequency of the sound wave, c is the speed of sound, η is the viscosity of the medium and ρ is the density of the medium.

It is assumed that the mixed medium is the sodium chloride solution, the largest component of SCGS brine. Substituting Eqs. (5) and (9) into Eq. (10), we have the viscous attenuation coefficient of sound wave in the mixed solution. Next, the emission frequency of sound wave was set to be in the range 100 kHz-1 MHz, the solution concentration to 2%, 4%, 6%, and 8%, and the solution temperature to 0-50°C. The viscous attenuation coefficients calculated for these parameters are given on the diagram in Fig. 3.

As shown in Fig. 3, when the frequency of the sound wave is in the range of 100 kHz-1 MHz, the viscous attenuation coefficient of the sound wave increases with the concentration of the mixed solution. When the concentration of the mixed solution remains constant, the coefficient increases with the frequency of the sound wave.

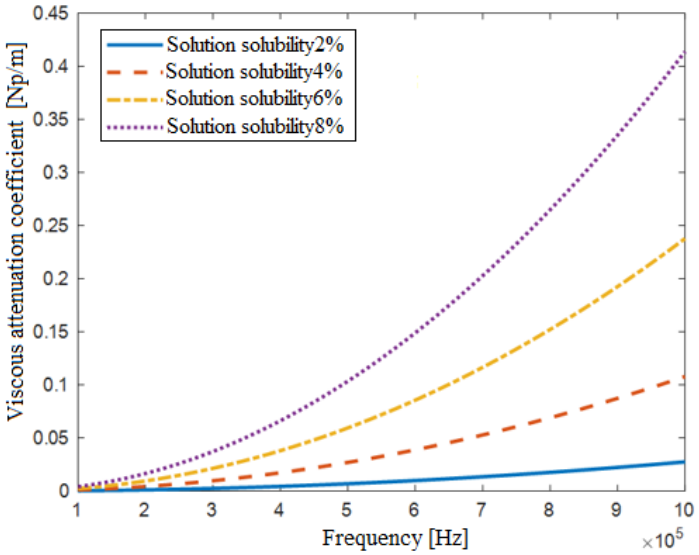

Fig. 3 Variation of the solution viscosity attenuation coefficient

3.2. Scattering Attenuation Features

The scattering attenuation of the sound wave stems from the uneven acoustic impedance of the material. In general, the scattering attenuation of the sound wave is calculated by the Rayleigh scattering theory. The scattering attenuation coefficient of the sound wave can be calculated by:

$$\alpha_s = \frac{8r^3 f^4 \pi^4}{3c^4} \tag{11}$$

where, r is the diameter of the insoluble particles, c is the speed of sound, f is the frequency of the sound wave.

Suppose the insoluble particles in the mixed medium are silica with a density of 2.2 g/cm^3, and the medium is water with a density of 1 g/cm^3. Substituting Eqs. (5) and (9) into Eq. (11), a formula for the scattering attenuation coefficient of the sound wave in the mixed solution is obtained. To display the scattering attenuation of the sound wave in the mixed media more intuitively, the parameter sensitivity analysis of sound wave scattering attenuation was carried out in MATLAB. Again, the emission frequency of the sound wave was set to 100 kHz-1 MHz, and the solution concentration to 2%, 4%, 6%, and 8%. The calculation results are shown in Fig. 4.

As shown in Fig. 4, the changing solution concentration exerts a slight impact on the scattering attenuation of the sound wave. The higher the wave frequency, the greater the scattering attenuation coefficient.

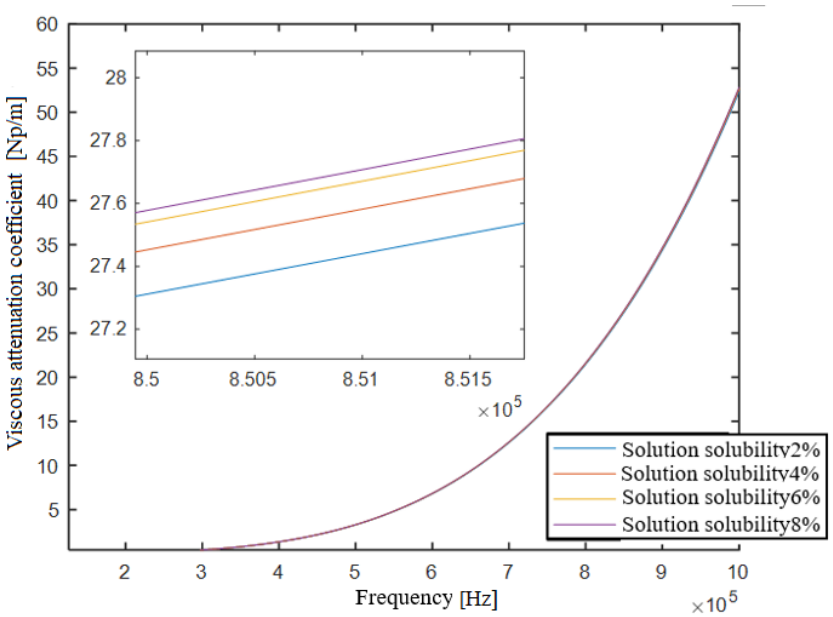

Fig. 4 The relationship between acoustic scattering attenuation and frequency

3.3. Thermal Attenuation Features

The thermal attenuation of sound waves is usually related to the thermal conductivity, constant volume specific heat, and constant pressure specific heat. The sound wave thermal attenuation coefficient can be calculated by:

$$\alpha_t = \frac{2\pi^2 f^2 x}{\rho c^3}\left(\frac{1}{C_V} - \frac{1}{C_P}\right) \tag{12}$$

where x is the thermal conductivity, C_v and C_p are the constant volume and constant pressure specific heat capacities, respectively, f is the frequency of the sound wave and c is the velocity of the sound wave.

To display the thermal attenuation of the sound wave more intuitively, the solution concentration was set to 2%-8% Substituting Eqs. (5) and (9) into Eq. (11), one obtains the formula for the thermal attenuation coefficient of the sound wave in the mixed solution. The parameter sensitivity analysis of sound wave thermal attenuation was carried out in MATLAB. The emission frequency of the sound wave was set to 100 kHz-1 MHz, the thermal conductivity to 0.65 W/m·°C, the constant pressure specific heat to C_p=10.392 kJ/kg°C, and the constant heat ratio k to 1.32. Then, $C_v = C_p/k$ = 7.873. The results are shown in Fig. 5.

As shown in Fig. 5, the thermal attenuation coefficient of the sound wave increases with the sound wave frequency. The larger the thermal attenuation coefficient, the slower the sound propagation. When the frequency remains constant, the solution is denser, the thermal attenuation coefficient is smaller and the sound propagation is faster.

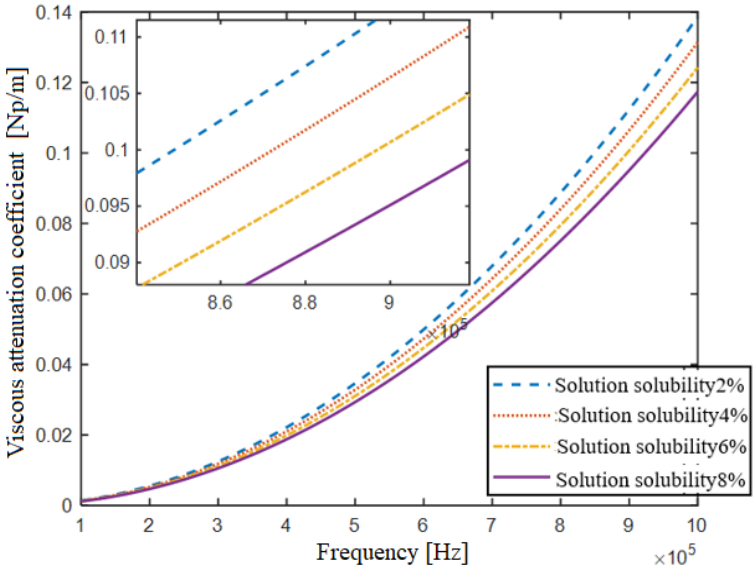

Fig. 5 Variation of thermal attenuation coefficient of acoustic with frequency

3.4. Total Attenuation Analysis

From the above analysis on three kinds of attenuations during sound wave propagation, it is clear that the attenuation mechanism is very complex when the sound wave passes through a mixed medium. Two or multiple attenuation forms may occur simultaneously, and act together on how the sound wave attenuates. According to the above theoretical calculation, scattering attenuation has the largest effect, while viscous attenuation and thermal attenuation have relatively small effects. When the wavelength of the propagating sound wave is much larger than the diameter of the particles in the medium, the attenuation of the ultrasonic wave in the mixed system can be directly added. The ultrasonic attenuation coefficient is expressed by the following formula [20]:

$$\alpha = \alpha_\eta + \alpha_s + \alpha_t = \frac{2\pi^2 f^2 \eta}{\rho c^3} + \frac{8r^3 f^4 \pi^4}{3c^4} + \frac{2\pi^2 f^2 x}{\rho c^3}\left(\frac{1}{C_V} - \frac{1}{C_P}\right) \tag{13}$$

where α_η is the viscous attenuation coefficient, α_s is the scattering attenuation coefficient, α_t is the thermal attenuation coefficient, while, c, P_{eff} and β_{eff} are given in Eqs. (5-7), respectively.

Substituting the solution concentrations of 2%, 4%, 6%, and 8% into Eq. (13), we obtained the change of the total attenuation of the sound wave in the suspension with different concentrations. The emission frequency of the sound wave was set to 100 kHz-1 MHz, the thermal conductivity to 0.65 W/m·℃, the constant pressure specific heat to C_p = 10.392 kJ/kg·℃, and the constant heat ratio k to 1.32. Then, C_v = C_p/k = 7.873. The results are shown in Fig. 6.

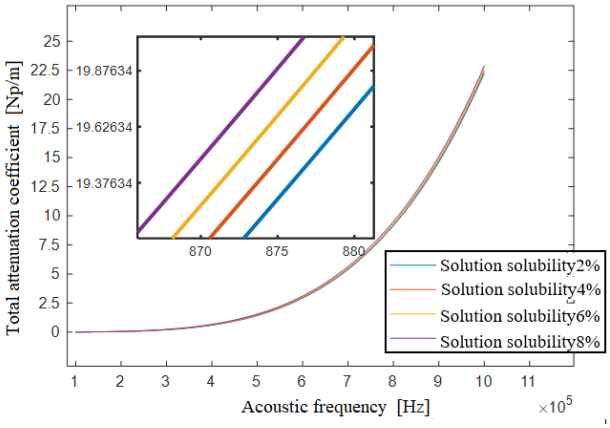

Fig. 6 Relationship between total attenuation coefficient of acoustic and frequency

It can be seen that the total attenuation coefficient of the sound wave in suspensions with different concentrations increases the frequency of the sound wave. When the frequency of the sound wave remains constant, the total attenuation coefficient of the sound wave increases with the suspension concentration. When the solution concentration is below 10%, the total attenuation coefficient of the sound wave depends on scattering attenuation, while viscous attenuation and thermal attenuation has little influence on the sound wave attenuation. Therefore, the scattering attenuation is regarded as the main attenuation form when the concentration of the suspension is less than 10%. In this case, the viscous and thermal attenuations are approximately negligible.

4. Experimental Analysis

To simulate the sound wave propagation in the complex environment of SCGS, the authors built an experimental platform and prepared different types of salt solutions (Fig. 7). On the platform, an ultrasonic apparatus drives the ultrasonic transducer to transmit and receive sound waves. The sound wave data were collected by external equipment and the experimental data were processed. The vessel and foam plates were kept warm by external heaters to keep the test temperature close to the set level, in order to reveal the sound wave attenuation.

a) 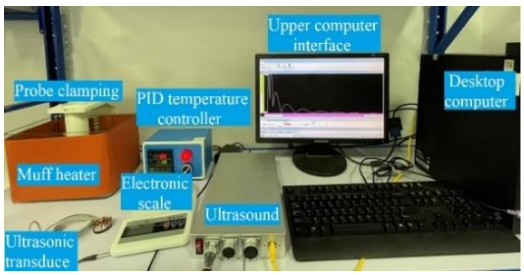

b) 

Fig. 7 Experimental platform (left) and different types of salts (right)

The ultrasonic attenuation coefficient was measured by calculating the relationship between amplitude and the propagation distance of two ultrasonic waves:

$$\alpha = -\frac{\ln(E/E_0)}{L} \tag{14}$$

where, E_0 is the amplitude of the first sound wave, E is the amplitude of the second sound wave, L is the distance between the ultrasonic transducer and the reflecting wall and it is a fixed value. The two amplitudes can also be determined by experiments. The above formula helps to solve the attenuation coefficient of the sound wave.

In the SCGS, the cavern is created through dissolution. Thus, the liquid medium of the cavern often covers various soluble salts, which are dissolved and mixed. This complicates the salt cavern medium. According to the existing surveys, the composition analysis of some salt mine media shows that the content of the same component varies significantly in salt mines at different places. Besides, different salt mines differ in the main components. In general, the primary content is sodium chloride, plus some salt solutions like potassium chloride, magnesium sulfate and calcium chloride. In our experiments, the sound attenuation features are examined with the four salt solutions as the objects.

First, the height of pure water was set to 160 mm, the distances between the ultrasonic transducers of different frequencies and the bottom surface of vessels to 145 mm (0.5 MHz), 117 mm (1 MHz), 127 mm (2 MHz), 127 mm (3.1 MHz), 129 mm (4 MHz), and 114 mm (5 MHz), in turn. Then, 131 g, 267 g, 409 g, and 557 g of sodium chloride were added to the solution, in turn. The resulting sodium chloride solutions were of the concentration of 2%, 4%, 6%, and 8%, respectively. After the sodium chloride was fully dissolved, the temperature of the solution was controlled to 20°C. For the ultrasonic transducer, the excitation voltage was set to 150 V, the pulse width to 80 ns, the sampling frequency to 2MHz, and the repetitive pulse frequency (RPF) to 2 kHz. The excitation frequency of the transducer was set to 0.5 MHz, 1 MHz, 2 MHz, 3.1 MHz, 4 MHz, and 5 MHz, in turn. The operating frequency of the ultrasonic transducer was obtained as 0.5 MHz, 1 MHz, 2 MHz, 3.1 MHz, 4 MHz, and 5 MHz, in turn. Once the solution temperature was stabilized, the mean of multiple measurements was taken. The results are listed in Table 1.

Table 1 Sonic data in different concentrations of sodium chloride solution

Medium concentration	peak	0.5 MHz Voltage [V]	1 MHz Voltage [V]	2MHz Voltage [V]	3.1 MHz Voltage [V]	4 MHz Voltage [V]	5 MHz Voltage [V]
2%	1	57.35	59.31	28.63	34.02	51.2	94.35
	2	19.64	15.8	5.23	5.1	6.87	14.21
4%	1	57.88	58.44	29.41	36.12	51.35	93.78
	2	19.21	16.52	5.48	5.1	5.98	12.45
6%	1	57.65	60.02	81.07	63.14	50.98	95.03
	2	15.74	10.12	9.13	6.45	4.57	9.67
8%	1	58.33	59.46	80.87	85.47	87.45	95.12
	2	12.57	9.15	7.88	7.54	6.72	8.54

It can be seen from Table 1 that the sound wave attenuation coefficient increased with the medium concentration. When the medium temperature remains constant, the coefficient increases with the sound wave frequency. Therefore, it is necessary to experimentally investigate the attenuation features of sound waves under the effect of changing temperature.

The solution was heated up to 50°C. During the heating process, the experimental data were recorded every for each temperature increment of 3°C. The operating frequency of the ultrasonic transducer was set to 0.5 MHz, 1 MHz, 2 MHz, 3.1 MHz, 4 MHz, and 5 MHz, in turn. The other settings remained the same as in earlier experiments. Once the solution temperature was stabilized, the mean of multiple measurements was taken. Figure 8 presents the results on sodium chloride solutions of the concentrations of 2%, 4%, 6%, and 8%, respectively. It can be learned that, when the concentration of sodium chloride solution remained constant, the sound wave attenuation coefficient is positively correlated with the solution temperature. The higher the temperature, the higher the sound wave attenuation coefficient, and the more serious the attenuation. However, the temperature had little effect on the attenuation of the sound wave in the sodium chloride solution. For every growth of 1°C in temperature, the attenuation coefficient of the sound wave increased by about 0.17 V/m. Giving overall consideration of concentration and temperature variations, the attenuation coefficient of the sound wave was the smallest in the sodium chloride solution, when the sound wave frequency was 0.5 and 1 MHz.

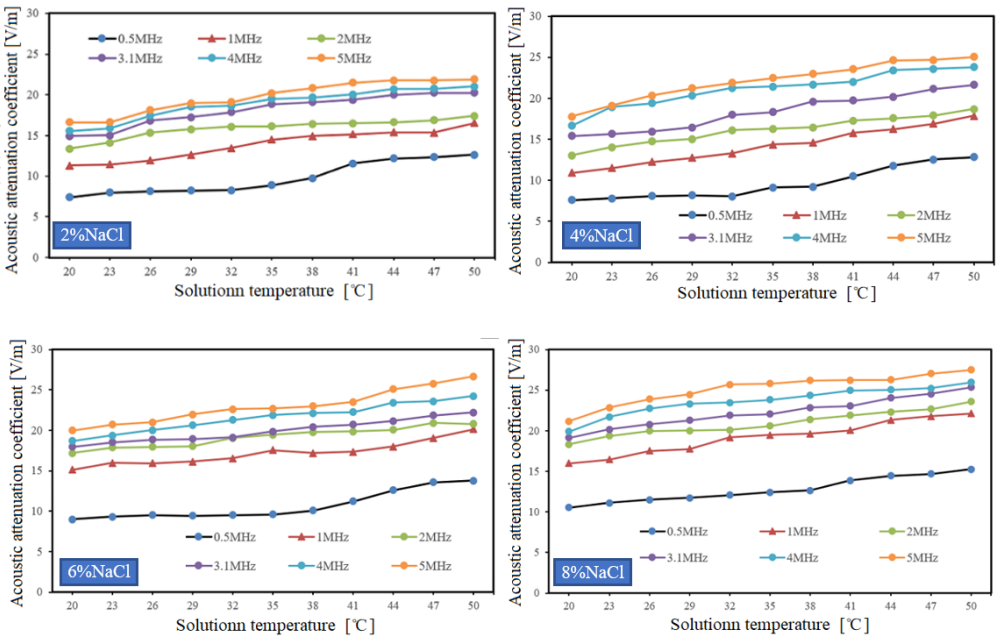

Fig. 8 Variation of acoustic attenuation coefficient in sodium chloride solution at different temperatures and concentrations

Without changing the above experimental conditions, sodium chloride was replaced with potassium chloride, magnesium sulfate and calcium chloride in turn for the subsequent experiments. Figure 9 reports the variation of sound wave attenuation coefficients in solutions of different concentrations.

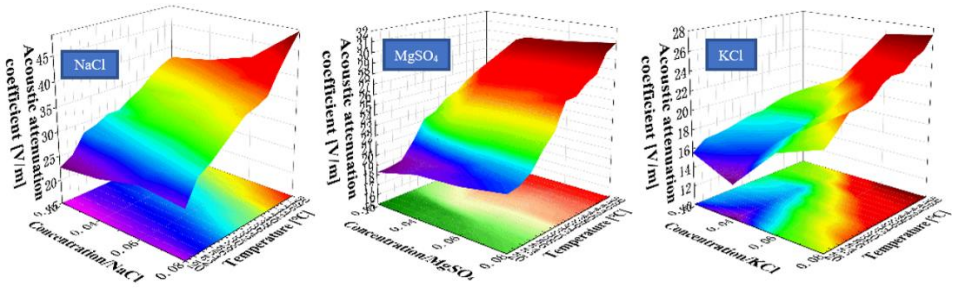

Fig. 9 Variation of acoustic attenuation coefficient in different concentrations solution

It can be seen from Fig. 9 that, when the medium temperature remains constant, the influence of medium concentration on sound wave attenuation features has a consistent trend with that of the sodium chloride solution. The sound wave attenuation coefficients are smallest at the wave frequencies of 0.5 MHz and 1 MHz, except for the case of sodium chloride solution.

Furthermore, the experimental data were extracted with solution concentrations of 2% and 6% (Fig. 10).

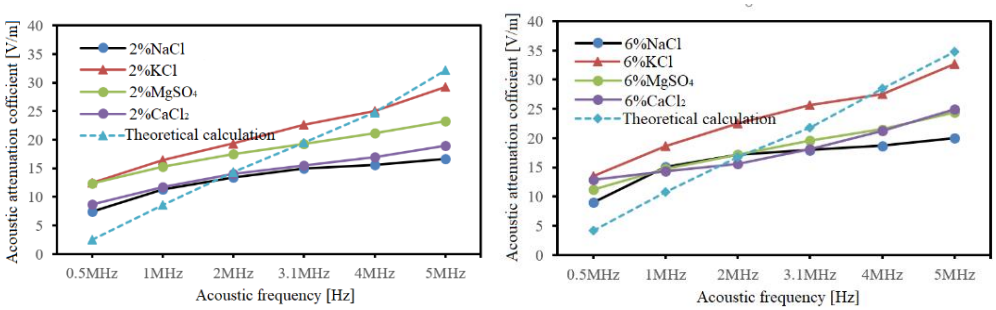

Fig. 10 Comparison of acoustic attenuation coefficients in different concentration solutions

As shown in Fig. 10, when the temperature remains the same, the different types of salt solutions of the same concentration can be ranked in descending order starting from potassium chloride solution, via magnesium sulfate solution and calcium chloride solution, to sodium chloride solution. Hence, the sound wave was attenuated most significantly in potassium chloride solution. In addition, the Urick model yields relatively accurate results when the sound wave frequency is high, indicating that the theoretical model has certain limitations in the calculation of sound wave attenuation in salt caverns.

Further experiments were conducted on the influence of temperature of sound wave attenuation features. Figure 11 shows the results based on the experimental data of 8% magnesium sulfate solution. The temperature influence over sound wave attenuation features in different solutions is the same as that in the case of sodium chloride solution. For different salt solutions, when the solution temperature rises by 1°C, the attenuation coefficient of the sound wave increases by about 0.83 V/m, 0.2 V/m, and 0.12 V/m in potassium chloride solution, magnesium sulfate solution, and calcium chloride solution, respectively. Overall,

temperature has the greatest influence on the attenuation of the sound wave in the potassium chloride solution, while the temperature influence on the other three solutions is similar.

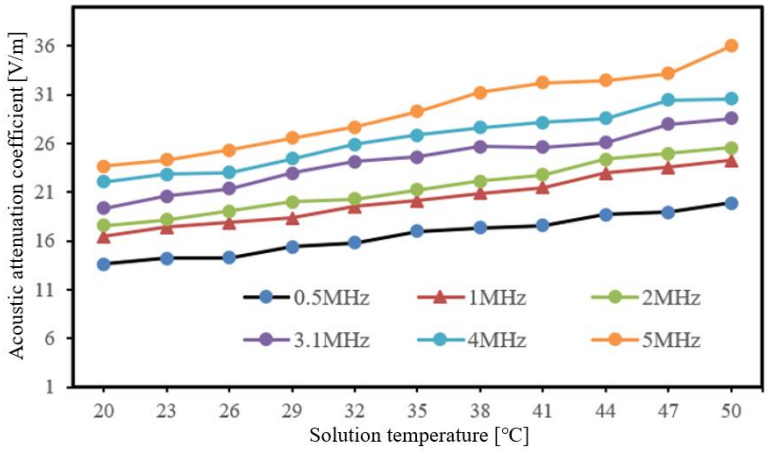

Fig. 11 Variation of sound attenuation coefficient in magnesium sulfate solution

5. CONCLUSIONS

This paper mainly theoretically analyzes the attenuation features of sound waves in salt cavities. Based on the Urick sound wave attenuation theory, the expression of sound velocity in dilute solution and the general empirical formula of solution density were added to study three attenuation forms of sound waves in dilute solutions with different concentrations. The following conclusions were drawn through theoretical and experimental analyses:

- When the solution concentration is less than 10%, the total attenuation coefficient of the sound waves depends on scattering attenuation, and the sound wave attenuation is not greatly affected by viscous attenuation and thermal attenuation.
- When the medium temperature remains the same, the sound wave attenuation coefficient increases with medium concentration, and sound wave frequency.
- The higher the temperature, the greater the sound wave attenuation. Temperature has the greatest effect on sound wave attenuation in potassium chloride solution. Overall, temperature has a small overall effect on the attenuation of sound waves.
- Among the four salt solutions, the most severe sound wave attenuation was observed in potassium chloride solution. The salt solutions can be ranked in descending order of sound wave attenuation coefficient as potassium chloride solution>magnesium sulfates solution > calcium chloride solution > sodium chloride solution.
- Without considering the distance requirement of sound wave detection, the sound wave attenuation obtained through theoretical and experimental analyses both reach a weak state at the sound wave frequencies of 0.5 and 1 MHz.

REFERENCES

1. Yang, C.H., Wang, T.T., Chen, H.S., 2023, *Theoretical and Technological Challenges of Deep Underground Energy Storage in China*, Engineering, 25(06), pp. 168-181.
2. Liu, Y., Li, Y., Ma, H., Shi, X., Zheng, Z., Dong, Z., Zhao, K., 2022, *Detection and evaluation technologies for using existing salt caverns to build energy storage*, Energies, 15, 9144.
3. Harker, A H., Temple, J.A.G., 2000, *Velocity and attenuation of ultrasound in suspensions of particles in fluids*, Journal of Physics D: Applied Physics, 21(11), 1576.
4. Prek, M., 2007, *Analysis of wave propagation in fluid-filled viscoelastic pipes*, Mechanical Systems and Signal Processing, 21(4), pp. 1907-1916.
5. Ross, J.L., 2010, *Ultrasonic waves in solids*, Science Press, 6(3), 87.
6. Queiros, R., Correa Alegria, F.C., Silva Girao, P., Cruz Serra, A.C., 2010, *Cross-correlation and sine-fitting techniques for high-resolution ultrasonic ranging*, IEEE Transactions on Instrumentation & Measurement, 59(12), pp. 3227-3236.
7. Hutchinson, B., Bevis, L.P., 2016, *Anomalous ultrasonic attenuation in ferritic steels at elevated tempera tures*, Ultrasonics, 69, pp. 268-272.
8. Hutchins, D.A., Watson, R.L., Davis, L.A.J., 2020, *Ultrasonic propagation in highly attenuating insulation materials*, Sensors, 20(8), 2285.
9. Li, R., Ni, Q.-Q., Xia, H., Natsuki, T, 2016, *Analysis of Individual Attenuation Components of Ultrasonic Waves in Composite Material Considering Frequency Dependence*, Composites Part B Engineering, 140, pp. 232-240.
10. Tsuji, K., Nakanishi, H., Norisuye, T., 2021, *Viscoelastic ECAH: Scattering analysis of spherical particles in suspension with viscoelasticity*, Ultrasonics, 115, 106463.
11. Yu, H., Tan, C., Dong, F., 2020, *Measurement of Particle Concentration by Multi-Frequency Ultrasound Attenuation in Liquid-Solid Dispersion*, IEEE Transactions on Ultrasonics, Ferroelectrics, and Frequency Control, 68(3), pp. 843-853.
12. Zhao, N.N., Xiao, X.Y., Fan, F.X., Su, M.X., 2022, *Ultrasonic attenuation model of mixed particle three-phase system based on Monte Carlo method*, Acta Phys. Sin, 70(7), 074303.
13. Yao, L., Zhang, Q.X., Wu, K., 2015, *Study on the attenuation laws of ultrasonic propagation in the inhomogeneous media*, in: Chan, K. (Ed.), Proceedings of the 2015 International Conference on Testing and Measurement: Techniques and Applications (TMTA 2015), 16-17 January 2015, Phuket Island, Thailand.
14. Fa, L., Li, L., Gong, H., Chen, W., Jiang, J., You, G., Liang, J., Zhang, Y., Zhao, M., 2022, *Investigation of the Physical Mechanism of Acoustic Attenuation in Viscous Isotropic Solids*, Micromachines, 13(9), 1526.
15. Shin, Y., 2019, *Signal attenuation simulation of acoustic telemetry in directional drilling*, Journal of Mechanical Science and Technology, 33, pp. 5189–5197.
16. Hu, J., Fu, L.Y., Wei, W., Zhang, Y., 2018, *Stress-Associated Intrinsic and Scattering Attenuation from Laboratory Ultrasonic Measurements on Shales*, Pure and Applied Geophysics, 175, pp. 929–962.
17. Grigorieva, N.S., Legusha, F.F., Safronov, K.S., 2023, *Scattering of a Plane Sound Wave by a Spherical Interface of Two Media with Sound Absorption in the Acoustic Boundary Layer*, Acoustical. Physics, 69, pp. 325-329.
18. Han, Q.B., Xu, S., Xie, Z.F., Ge, R., Wang, X., Zhao, S.Y., Zhu, C.P., 2013, *Analysis and experimental verification of the relation between Scholte wave velocity and sediment containing two-phase fluid properties*, Acta Phys. Sin,, 62(19), 194301.
19. Yang, H.Y., Wang, Y., Dai, Y., Zhang, J.F., Chen, G., 2023, *On the acoustic attenuation characteristics of sonar detection in the salt-cavern gas storage environment*, Frontiers in Earth Science,10, 10299446.
20. Fan, J., Wang, F., 2021, *Review of ultrasonic measurement methods for two-phase flow*, Review of Scientific Instruments, 92(9), 091502.